LIMNOLOGY and OCEANOGRAPHY

Higher temperature, increased CO₂, and changing nutrient ratios alter the carbon metabolism and induce oxidative stress in a cosmopolitan diatom

Hugo Duarte Moreno [ORCID],[1]* Sebastian Rokitta [ORCID],[2] Nelly Tremblay [ORCID],[1,3] Maarten Boersma [ORCID],[1,4] Elisabeth Groß [ORCID],[1] Helena C. L. Klip [ORCID],[1,5] Karen H. Wiltshire [ORCID],[6] Cédric L. Meunier [ORCID][1]

[1]Alfred-Wegener-Institut, Helmholtz-Zentrum für Polar-und Meeresforschung, Biologische Anstalt Helgoland, Germany
[2]Alfred-Wegener-Institut, Helmholtz-Zentrum für Polar-und Meeresforschung, Bremerhaven, Germany
[3]Département de biologie, chimie et géographie, Université du Québec à Rimouski, Rimouski, Canada
[4]University of Bremen, Bremen, Germany
[5]Flathead Lake Biological Station, University of Montana, Polson, Montana, USA
[6]Alfred-Wegener-Institut, Helmholtz-Zentrum für Polar- und Meeresforschung, Wattenmeerstation, List auf Sylt, Germany

Abstract

Phytoplankton are responsible for about 90% of the oceanic primary production, largely supporting marine food webs, and actively contributing to the biogeochemical cycling of carbon. Yet, increasing temperature and pCO₂, along with higher dissolved nitrogen: phosphorus ratios in coastal waters are likely to impact phytoplankton physiology, especially in terms of photosynthetic rate, respiration, and dissolved organic carbon (DOC) production. Here, we conducted a full-factorial experiment to identify the individual and combined effects of temperature, pCO₂, and N : P ratio on the antioxidant capacity and carbon metabolism of the diatom *Phaeodactylum tricornutum*. Our results demonstrate that, among these three drivers, temperature is the most influential factor on the physiology of this species, with warming causing oxidative stress and lower activity of antioxidant enzymes. Furthermore, the photosynthetic rate was higher under warmer conditions and higher pCO₂, and, together with a lower dark respiration rate and higher DOC exudation, generated cells with lower carbon content. An enhanced oceanic CO₂ uptake and an overall stimulated microbial loop benefiting from higher DOC exudation are potential longer-term consequences of rising temperatures, elevated pCO₂ as well as shifted dissolved N : P ratios.

Phytoplankton are responsible for about 90% of total oceanic primary production (Duarte and Cebrián 1996), making them major contributors to the biogeochemical cycling of carbon (Buesseler 1998; Bowler et al. 2010). Two distinct marine

carbon pools derive directly from the biological activity of photosynthetic organisms: particulate organic carbon (POC), bound in cell biomass, and dissolved organic carbon (DOC), released by living phytoplankton or decaying cells, through sloppy feeding of grazers, consumption, and excretion by higher trophic levels or viral lysis (Jiao et al. 2010). Once fixed as phytoplankton biomass, carbon can be transferred via trophic processes through the food web or sink to the deep sea (Honjo and Manganini 1993). These fluxes are essential components of biogeochemical cycling and the "marine organic carbon pump" and are influenced by phytoplankton cellular physiological processes.

After inorganic carbon is assimilated into carbohydrates through photosynthesis, it can take different pathways in a phytoplankton cell: the carbon can be used for storage and growth; it can be remineralized for mitochondrial energy generation and fuel cellular processes; or it can be exuded in the form of organic molecules (Marra and Barber 2004; Tortell et al. 2008; Thornton 2014). The relative proportions of these

intracellular carbon fluxes are directly influenced by environmental conditions, such as temperature, partial pressure of carbon dioxide ($p\mathrm{CO_2}$), and concentration of dissolved nutrients (Neori and Holm-Hansen 1982; Alipanah et al. 2015; Padfield et al. 2016), all of which have experienced large perturbations due to human activities. Indeed, anthropogenic $\mathrm{CO_2}$ emissions and the resulting increase in atmospheric $p\mathrm{CO_2}$ contribute to the greenhouse effect, that is, global warming. In addition, part of this $\mathrm{CO_2}$ dissolves into the ocean, and lowers seawater pH, leading to ocean acidification (Doney et al. 2009; Anderson et al. 2016). Human activities have also altered dissolved nutrient concentrations through nutrient runoffs, leading to coastal waters' enrichment by nitrogen and phosphorus. To minimize the impacts of eutrophication, European governments have applied different methods to reduce nutrient loads into coastal waters. These strategies have been more effective at reducing nitrogen than phosphorus runoffs, causing not only a general reduction of dissolved inorganic nutrient concentrations, but also an increase of the N : P ratio, at least well documented in the North Sea (Grizzetti et al. 2012), thus increasing the potential of P limitation for phytoplankton (Peñuelas et al. 2013).

Increasing aqueous $\mathrm{CO_2}$ concentrations could have positive effects on primary producers that profit from the higher availability of $\mathrm{CO_2}$ (Bach et al. 2019). However, other studies have shown that responses of phytoplankton to increasing oceanic $p\mathrm{CO_2}$ may be complex (Beardall and Raven 2004; Taucher et al. 2015; Alvarez-Fernandez et al. 2018), and the consequences for photosynthesis and wider phytoplankton ecophysiology remain to be clarified. Studies have found different effects of warming and ocean acidification on various physiological processes related to carbon metabolism in phytoplankton, including increase in photosynthesis and respiration rates (Wu et al. 2010; Goldman et al. 2017), higher DOC production (Engel et al. 2010), and downregulation of carbon-concentrating mechanisms (Thangaraj and Sun 2021; Rokitta et al. 2022). Environmental ratios of dissolved inorganic N : P influence cellular quotas of POC, photosynthetic and growth rate in phytoplankton (Rasdi and Qin 2014; Li and Sun 2016), as well as DOC exudation (Obernosterer and Herndl 1995). The uncertainties about the interactions of environmental drivers and the co-dependency of cellular carbon pathways on different environmental drivers make the responses of phytoplankton cells to future environmental change even more difficult to predict (Gao and Campbell 2014; Wolf et al. 2019).

Environmental conditions modulate the rates of respiration and photosynthesis in phytoplankton (Hancke et al. 2008; Padfield et al. 2016), and the associated electron transport rates which determine the degree of reduction of the electron transport chains (ETCs) in chloroplasts and mitochondria (Mittler et al. 2004; Janknegt et al. 2008). When ETCs are overreduced, electrons can "leak" and react with free $\mathrm{O_2}$, extensively generated as a photosynthesis by-product, creating superoxide radicals ($\mathrm{O_2^{-\bullet}}$) (Gechev et al. 2006). This primary reactive oxygen species (ROS) is further converted into other oxidative compounds, such as hydrogen peroxide ($\mathrm{H_2O_2}$) and the highly reactive hydroxyl radical ($\mathrm{HO^{\bullet}}$), which are able to cause oxidative damage to lipids, proteins, and DNA (Halliwell 1987). Oxidative damage can lead to loss of photosynthetic capacity, due to membrane lipid peroxidation, lower growth rates as well as decreased chlorophyll a (Chl a) content (Rajagopal et al. 2000; Mallick et al. 2002; Yu et al. 2004). Phytoplankton can apply different strategies to prevent the formation of ROS and combat such compounds when their formation cannot be avoided. In the chloroplast, excess light absorbed by the antenna complex can be quenched as thermal energy by activating the xanthophyll cycle (Janknegt et al. 2008), while the proportions of photoprotective vs. light-harvesting pigments can be rearranged to better tune energy flow to the photosystems (Dubinsky and Stambler 2009). Activation of the alternative oxidase (AOX) pathway within the mitochondria can relieve electron flow through the ETC to prevent leakages, yet at the cost of lowered ATP production by dark respiration (Day and Wiskich 1995; Allen et al. 2008). Antioxidant enzymes also play an important role in scavenging ROS. Superoxide dismutases (SODs) are potent antioxidants widely utilized to catalyze the dismutation of $\mathrm{O_2^{-\bullet}}$ into $\mathrm{O_2}$ and $\mathrm{H_2O_2}$ (Janknegt et al. 2008). Once formed, $\mathrm{H_2O_2}$ can be further decomposed into harmless $\mathrm{O_2}$ and $\mathrm{H_2O}$ by other enzymes, such as catalase (CAT) and glutathione peroxidase (GPx) (Barros et al. 2003; Vega-López et al. 2013). While several studies have reported modulation of antioxidant response and oxidative stress by temperature, $p\mathrm{CO_2}$, and dissolved nutrient concentrations in different classes of photosynthetic organisms (Lesser 1997; Choo et al. 2004; Yakovleva et al. 2009; Gillespie et al. 2011; Brutemark et al. 2015; Kvernvik et al. 2020), the potential interactions between these environmental factors affecting the antioxidant capacity of marine phytoplankton remain poorly understood.

In this study, we tested the influence of temperature, $p\mathrm{CO_2}$, and dissolved N : P ratios on the cellular carbon fluxes and antioxidant response of the diatom *Phaeodactylum tricornutum*. Overall, our work assesses how multiple global change drivers may act separately and in combination to influence physiological processes related to carbon metabolism, mainly primary production, respiration and DOC production. These processes involve electron transfer chains in chloroplasts and mitochondria and are directly related to the formation of ROS in phytoplankton cells. Therefore, we also assessed the antioxidant response and oxidative stress in parallel to potential changes in carbon metabolism.

Materials and methods

A full-factorial design was applied to test the influence of two $\mathrm{CO_2}$ partial pressures (400 and 1000 μatm), temperatures (18°C and 21°C), and N : P ratios of dissolved inorganic nutrients (16 and 25 mol $\mathrm{L^{-1}}$), forming eight independent treatments in quadruplicates. The $p\mathrm{CO_2}$ levels were chosen to represent the contemporary and the RCP 8.5 scenario

atmospheric pCO_2 based on predictions of CO_2 emissions by the Intergovernmental Panel on Climate Change for the end of the 21st century (IPCC 2021). 18°C is the mean temperature value for summer (July–August) at the Helgoland roads time-series station (North Sea) and 21°C represents the +3.0°C increase expected according to the RCP 8.5 scenario. These temperatures are in the range of the maximum growth rate of this species, which has been found to be around 20°C (Kudo et al. 2000; Kvíderová and Lukavský 2003; Bitaubé Pérez et al. 2008). We included different nutrient regimes to this experiment as well. The N : P of 16 represents the balanced Redfield ratio, while an N : P of 25, achieved by lowering the concentrations of dissolved P, resembles the increasing P limitation predicted for the future. The model diatom *P. tricornutum* was chosen as it is native to the North Sea and does not form chains, which allowed us to precisely determine cell concentrations by flow cytometry. This diatom has a worldwide distribution and is common in coastal waters (Hendey 1964). Despite the uncommon capacity of this diatom to grow in the absence of silica (Hendey 1954), the sequencing of its genome, as well as multiple ecophysiological studies, identified this species as a model organism representative of the Bacillariophyceae group (Oudot-Le Secq et al. 2007; Bowler et al. 2008; Martin-Jézéquel and Tesson 2013). Nevertheless, the use of a single diatom strain for this experiment (CCAP 1052/1A) might limit the applicability of our results to other strains or species. In the laboratory, phytoplankton strains become adapted overtime to the artificial environments they grow in, and their response may differ from natural conditions or other isolated strains (Lakeman et al. 2009). Carbon fluxes were measured through the rates of primary production, dark respiration, DOC production and POC contents, representing organic carbon production, organic carbon consumption, organic carbon exudation, and organic carbon in the cells biomass, respectively. The antioxidant response was assessed based on different biomarkers, including the contents of protective carotenoids (β-carotene, diadinoxanthin and violaxanthin), the prevalence of the AOX pathway, antioxidant enzyme activities (CAT, manganese superoxide dismutase [SOD-Mn], GPx, glutathione *S*-transferase [GST]), and by determination of malondialdehyde (MDA) formation as a proxy for oxidative damage to membrane lipids.

Culture conditions

Cultures of *P. tricornutum* (Strain CCAP 1052/1A) were grown at 18°C or 21°C in a temperature-controlled room in 2 L glass bottles (Duran) closed with airtight lids. The cultures were grown in F/20 medium (Guillard 1975) prepared with artificial seawater according to the protocol of Harrison et al. (1980), modified by Berges et al. (2001), and sterile filtered (0.2 μm) to avoid contamination. Total alkalinity (TA) was adjusted by the addition of NaOH until it reached natural seawater levels ($\sim$ 2350 μmol kg SW^{-1}). To yield N : P ratios of 16 and 25, nitrate was added to reach a concentration of 88 μmol NO$_3$ L^{-1}, and phosphate concentrations in the

growth medium were set to 5.5 μmol PO$_4$ L^{-1} and 3.5 μmol PO$_4$ L^{-1}, respectively (Supporting Information Fig. S1). The pCO_2 of the medium was adjusted by bubbling it for 24 h with air mixtures containing either 400 or 1000 μatm CO_2, which were obtained from a CO_2-mixing system (GDZ 401; Schoo et al. 2013). Cultures were irradiated with 100 μmol photons m^{-2} s^{-1} by LED light bars (Mitras 2 Daylight; GHL) under a 14 : 10 h light : dark cycle. The culture bottles were continuously rotated on a roller table to prevent cell sedimentation. The diatom cultures were pre-acclimated to every treatment for at least 20 generations. The experiment was subdivided into two periods. In the first period of 4 d, we measured DOC production and POC, whereas the second period was focused on the measurements of antioxidant response, pigments, and rates of photosynthesis and respiration. Samples for production rates of DOC were collected daily over a 4-d period during the first incubation phase, following the acclimation period (20 generations). Samples for POC were collected on the last day of the first incubation phase. Initial cell concentration was always $\sim$ 400 cells mL^{-1}. After the first incubation phase of 4 d, cells were diluted back to 400 cells mL^{-1} with described media and grown for a second incubation phase of 4 d to acquire more biomass for further measurements. On the last day of the second incubation phase, cells were harvested for assessments of dark respiration, primary production, AOX activity, antioxidant enzyme assays, and MDA concentration, as well as for the analyses of pigments as indicators of antioxidant capacity and photoprotective capacities. Cultures were kept dilute to avoid self-shading, fluctuations in pH during the experiment, and drifts in carbonate chemistry. Cells were harvested at dilute concentration during the exponential growth phase well before 10% of the dissolved inorganic carbon (DIC) in the culture was consumed. This measure ruled out DIC limitation, drifts in carbonate chemistry as well as NO$_3$ and PO$_4$ depletion. This limit was ascertained by modeling the carbonate system with the help of the CO_2SYS Excel Macro (Pierrot et al. 2006).

Seawater carbonate system and dissolved macronutrients

The seawater carbonate system was calculated based on determined DIC, pH, temperature, and salinity using the CO_2SYS Excel Macro (Pierrot et al. 2006) with acidity constants defined by Mehrbach et al. (1973) refitted by Dickson and Millero (1987). Salinity was measured with a salinometer (WTW Cond 3110 SET 1) directly from TA samples. An aliquot of each culture was taken daily to measure pH with a WTW Tetracon® 925 probe. Samples for dissolved inorganic nutrients, salinity, TA and DIC were taken from the medium before cell inoculation, and on the last day of each incubation phase. TA samples were taken by filling an airtight 100 mL transparent glass bottle, avoiding air bubbles, with a filtered culture medium (GF/F filter 0.45 μm; Whatman). The samples were stored at 4°C before analysis through linear Gran-titration (Dickson 1981) using a TitroLine alpha plus (Schott). Samples for DIC were filtered through 0.45 μm polytetrafluoroethylene

(PTFE) filters and kept in 5 mL brown glass bottles, free of air bubbles, at 4°C before analysis with the colorimetric method of Stoll et al. (2001). Dissolved inorganic nutrients (DIP = PO_4^{3-} and DIN = NO_x) samples were kept frozen at $-20°C$ until being measured with a continuous-flow analyzer (QuAAtro39; Seal Analytical) according to Strickland and Parsons (1972). Results of dissolved inorganic nutrient analyses and seawater carbonate chemistry are available as Supporting Information Fig. S1 and Supporting Information Table S1, respectively. There was not enough biomass growth during the experiment to exhaust the dissolved nutrient supply. Thus, the cells did not face nutrient limitations during the experiment (Supporting Information Fig. S2).

Photosynthesis and dark respiration rate

Photosynthesis and dark respiration rates were measured as net O_2 evolution rates. We used a high-resolution O_2k-FluoRespirometer (Oroboros Instruments) calibrated with each treatment medium. The 2 mL incubation chambers of the respirometer are airtight, temperature controlled, and equipped with magnet stirrers to keep the cells in suspension. To acquire enough cells to reach rates within the equipment resolution, cells were concentrated by gently filtering 100–200 mL of each culture on a polycarbonate filter (0.45-μm pore size) with a suction pressure lower than 200 mbar relative to the atmosphere. The volume used depended on cell concentration in the culture. Concentrated phytoplankton cells were resuspended in 5 mL of 30 μmol L^{-1} 4-(2-hydroxyethyl)-1-piperazineethanesulfonic acid-buffered culture medium to maintain constant pH during the measurements. This aliquot was dark acclimated in the instrument for 10 min at the respective experimental temperatures before applying a rapid light curve (RLC), where the aliquot was exposed for 10 min to irradiance of 50, 100, 150, and 300 μmol photons m^{-2} s^{-1} provided by LEDs. A last light intensity step of 600 μmol photons m^{-2} s^{-1}, was provided by a Zeiss/Schott CL 1500 ECO lamp. Each light step was followed by 10 min of darkness to account for variation in dark respiration due to a higher photosynthetic rate. Dark respiration was calculated as the mean of all respiration measurements taken during every dark period. To quantify carbon fluxes, O_2 fluxes were converted into CO_2 fluxes using a photosynthetic quotient of 1.56 and a respiratory quotient of 0.6 determined for *P. tricornutum* (Wagner et al. 2006). We used least-squares fitting on the obtained data to derive physiological photosynthesis parameters, such as compensation point, as well as photochemical efficiency (α), light acclimation index (I_k) and maximum net photosynthesis rate ($V_{\max}$), following equations from Rokitta and Rost (2012). The compensation point obtained in the procedure represents the irradiance where the respiration rate is equal to the photosynthesis rate. α is the initial slope of the RLC and indicates the efficiency of light energy conversion into chemical energy via photosynthesis. I_k represents the irradiance where photosynthesis transitions into saturation and

$V_{\max}$ shows the highest electron transport rate attained during the RLC. Raw data of the RLC are available in the Supporting Information Fig. S3.

Determination of growth rates, elemental quotas, and DOC production

Cell concentrations were measured by flow cytometry (BD Accuri C6 Plus; BD Biosciences) with 100 μL samples processed at a flow rate of 35 μL min^{-1}. The specific growth rate (μ) was calculated as:

$$\mu = (\ln_{C1} - \ln_{C0}) \times \Delta t^{-1},$$

where C_0 and C_1 are the initial and final cell concentrations and Δt is the time interval in days. The growth rate was calculated based on cell concentrations on the initial and final day of each incubation phase and computed as mean of both incubation phases, generating one growth rate value per replicate.

Samples for POC were taken by filtering 200 mL of each phytoplankton culture on precombusted (12 h, 500°C) GF/F filters (0.45 μm; Whatman), with suction pressure of 200 mbar relative to the atmosphere. The filters were then soaked with 200 μL of 0.2 mol L^{-1} HCl to remove any calcite or other inorganic carbon contaminants, and dried in an oven at 60°C. The filter acidification ensured that of all carbon measured on the filters was the carbon contained in the phytoplankton cells. Carbon content on the filters was determined with an elemental analyzer (Vario Micro Cube; Elementar).

To quantify DOC, samples of 20 mL were collected from the artificial seawater batch produced to prepare the medium before cells' incubation (initial), and from every culture bottle on the final day of the first incubation. Samples were collected with a sterile plastic syringe and filtered through a 0.45 μm PTFE filter. The first 2 mL of the sample was used to rinse the filter and were discarded. The samples were collected in technical duplicates and stored in HCl washed and precombusted glass vials. Samples were acidified with HCl and kept at $-20°C$ until analysis. DOC was determined by high-temperature catalytic oxidation and subsequent nondispersive infrared spectroscopy and chemiluminescence detection, automatically conducted in a TOC-L$_{CPH/CPN}$ analyzer (Shimadzu). Net DOC production per cell (D) was calculated based on the following formula derived from the integral of total DOC production in the culture and cell growth:

$$D = \frac{\mathrm{DOC}_p}{C_0} \times \frac{\mu}{\left(\frac{C_1}{C_0} - 1\right)},$$

where DOC_p is the total DOC production in the culture over the whole incubation period (pmol mL^{-1}), C_0 and C_1 are the initial and final phytoplankton cell concentrations (cells mL^{-1}),

and μ is the specific growth rate (d^{-1}; *see* Supporting Information S1 for the integral resolution).

We chose not to work with axenic cultures to avoid the potential effects of the absence of a microbiome in the culture, which interacts with phytoplankton in natural conditions (Stock et al. 2019). We also wanted to avoid the negative impacts that antibiotics would have had on phytoplankton physiology (Siedlewicz et al. 2020), if we had decided to sterilize the cultures. Therefore, to account for bacterial DOC consumption, 200 mL of each culture was filtered through a polycarbonate filter (3-μm pore size; Millipore) to remove phytoplankton cells, and subsequently filtered through a polycarbonate filter (0.45-μm pore size). The bacterial cells captured on the 0.45-μm filter were resuspended and incubated in an O$_2$k-FluoRespirometer to measure their respiration rate for the phytoplankton cells (*see* above). This procedure ensured enough bacterial cell biomass for accurate measurements. The aliquots of each incubation for respirometry were also subsequently preserved to determine bacterial cell concentrations. The bacterial respiration rate (pmol O$_2$ cell^{-1} d^{-1}) was also converted to C consumption using an average respiratory quotient of 1.55 (Allesson et al. 2016), and the bacterial carbon consumption was added to the phytoplankton DOC production since DOC is the carbon source for bacteria in the culture. Bacterial DOC consumption (DOC$_c$) was calculated using the formula:

$$\text{DOC}_c = \frac{B_0 \times \left({}^{B_1}/_{B_0} - 1 \right) \times C}{\mu},$$

where c is the bacterial respiration rate (pmol C cell^{-1} d^{-1}), B_0 and B_1 are the bacterial cell initial and final concentrations in the cultures (cells mL^{-1}), and μ is the specific bacterial growth rate (d^{-1}) based on the initial and final bacterial cell concentration in the culture and calculated as for phytoplankton. Data on bacterial biomass used for the calculation of DOC consumption is available in the Supporting Information Fig. S4.

Bacterial cell concentration was also determined from each phytoplankton aliquot incubated in the respirometer for photosynthesis and dark respiration rates to ensure that bacterial biomass accounted for less than 10% of the total carbon biomass. These samples were fixed with glutaraldehyde (0.1% final concentration) and frozen at −80°C until analysis. The samples were thawed in a water bath (20°C) and stained with SYBR Green (Invitrogen) as described in Marie et al. (2005). Bacterial cells were quantified by processing the samples through flow cytometry (BD Accuri™ C6 Plus; BD Biosciences) at a flow rate of 12 μL min^{-1} for 1–2 min. Samples were diluted with sterile filtered seawater (0.2 μm) when flow cytometry events were higher than 400 events s^{-1}. Bacteria cell counts were converted into carbon using the 20 fg C cell^{-1} factor defined by Lee and Fuhrman (1987). Nevertheless,

bacteria concentration was low, representing on average 11.6% of total carbon biomass in the culture on the harvesting day and less than 5% during measurements with the respirometer.

Enzyme assays and pigment detection

A concentrated phytoplankton aliquot (obtained as described in "Photosynthesis and dark respiration rate") was incubated in the two chambers of the O$_2$k-FluoRespirometer (Oroboros Instruments). AOX activity was determined using Substrate-uncoupler-inhibitor titration (SUIT, 022 www.bioblast.at/index.php/SUIT-022_O2_ce_D051 and 023 www.bioblast.at/index.php/SUIT-023_O2_ce_D053) protocols specifically developed to distinguish between oxygen consumption derived from mitochondrial AOX and from respiratory complex IV (CIV). As a first step, routine dark respiration was measured for both chambers. Then, one of the chambers was used to quantify AOX-dependent respiration after inhibition of CIV with 1 mmol L^{-1} potassium cyanide (KCN), while the other was used for CIV dependent respiration after inhibition of AOX with 1 mmol L^{-1} salicylhydroxamic acid (SHAM). We expressed AOX as the ratio between SHAM-inhibited respiration rate and routine respiration (AOX : Resp). The AOX : Resp ratio indicates the proportion of electrons that ends up in the AOX pathway compared to all electrons used during the dark respiration process.

Samples for the assessments of antioxidant enzyme activities and MDA as an oxidative stress marker were collected by filtering 200–250 mL of the culture through a polycarbonate membrane filter (3-μm pore size; Millipore) to concentrate cells. The cells caught on the filter were resuspended in culture medium, transferred into a 1.5 mL assay reaction tube (Eppendorf) and centrifuged at 27,000 RCF for 3 min at treatment temperature to form a cell pellet. Then, the supernatant was removed and the phytoplankton cells were immediately frozen in liquid N$_2$ and kept at −80°C until analysis. For determination of MDA, the samples were thawed and homogenized in 250 μL of 1.1% H$_3$PO$_4$ (Mixer Mill MM301; Retsch) for 1 min with the frequency of 30 rotations s^{-1}. Measurements of MDA content were done in triplicate according to Uchiyama and Mihara (1978).

To quantify the antioxidant enzyme activities and soluble proteins, samples were homogenized with 125 μL of phosphate buffer solution (50 mmol L^{-1} potassium phosphate dibasic and monobasic mixture [K$_2$HPO$_4$/KH$_2$PO$_4$], 50 mmol L^{-1} ethylenediaminetetraacetic acid [EDTA], 1 mmol L^{-1} phenylmethylsulfonyl fluoride [PMSF; C$_7$H$_7$FO$_2$S], pH 7.5) and centrifuged at 27,000 RCF for 5 min at 4°C. The same supernatant extract was measured in technical triplicates for CAT following Aebi (1984), SOD-Mn following Suzuki (2000), GPx following Ahmad and Pardini (1988), and GST following the protocol from Habig and Jakoby (1981). Soluble protein contents were

Table 1. Statistical results of three-way ANOVA models indicating treatment effects.

Variable	Factor 1	Factor 2	Factor 3	MS	F	p Value	Effect indicated by Tukey's post hoc test
Primary production	Temperature	–	–	0.819	9.918	**0.004***	Higher at 21°C
	–	$p\text{CO}_2$	–	0.401	4.854	**0.037***	Higher at 1000 $p\text{CO}_2$
	–	–	N : P	0.194	2.348	0.138	–
	Temperature	$p\text{CO}_2$	–	0.152	1.843	0.187	–
	Temperature	–	N : P	0.301	3.644	0.068	–
	–	$p\text{CO}_2$	N : P	0.052	0.632	0.434	–
	Temperature	$p\text{CO}_2$	N : P	0.036	0.435	0.516	–
Dark respiration rate	Temperature	–	–	0.061	30.34	**< 0.001***	Lower at 21°C
	–	$p\text{CO}_2$	–	0.005	2.406	0.134	–
	–	–	N : P	0.005	2.297	0.143	–
	Temperature	$p\text{CO}_2$	–	0.065	30.86	**< 0.001***	Lower dark respiration rate at 21°C when $p\text{CO}_2$ is 1000
	Temperature	–	N : P	0.005	2.688	0.114	–
	–	$p\text{CO}_2$	N : P	0.006	3.158	0.088	–
	Temperature	$p\text{CO}_2$	N : P	0.001	0.659	0.425	–
DOC production	Temperature	–	–	7.276	400.2	**< 0.001***	DOC exudation at 21°C and DOC uptake at 18°C
	–	$p\text{CO}_2$	–	0.010	0.523	0.476	–
	–	–	N : P	0.128	7.023	**0.014***	Higher DOC production when N : P is 25
	Temperature	$p\text{CO}_2$	–	0.173	9.542	**0.005***	Higher DOC production at 21°C when $p\text{CO}_2$ is 1000
	Temperature	–	N : P	0.001	0.054	0.817	–
	–	$p\text{CO}_2$	N : P	0.029	1.602	0.218	–
	Temperature	$p\text{CO}_2$	N : P	0.020	1.127	0.299	–
Particulate organic carbon	Temperature	–	–	1.096	272.8	**< 0.001***	Lower at 21°C
	–	$p\text{CO}_2$	–	0.023	5.728	**0.025***	Lower at 1000 $p\text{CO}_2$
	–	–	N : P	0.001	0.378	0.545	–
	Temperature	$p\text{CO}_2$	–	0.015	3.685	0.067	–
	Temperature	–	N : P	0.027	6.730	**0.016***	Lower carbon content at 21°C when N : P is 25
	–	$p\text{CO}_2$	N : P	0.013	3.282	0.083	–
	Temperature	$p\text{CO}_2$	N : P	0.001	0.135	0.717	–
Growth rate	Temperature	–	–	0.035	38.71	**< 0.001***	Higher at 21°C
	–	$p\text{CO}_2$	–	0.001	0.266	0.610	–
	–	–	N : P	0.002	1.946	0.176	–
	Temperature	$p\text{CO}_2$	–	0.014	15.39	**< 0.001***	No significant increase at 21°C when $p\text{CO}_2$ is 1000
	Temperature	–	N : P	0.001	0.857	0.364	–
	–	$p\text{CO}_2$	N : P	0.008	8.427	**0.008***	Higher growth rate at 1000 $p\text{CO}_2$ when N : P is 25
	Temperature	$p\text{CO}_2$	N : P	0.001	0.204	0.656	–
Compensation point	Temperature	–	–	31.81	44.74	**< 0.001***	Lower at 21°C
	–	$p\text{CO}_2$	–	0.170	0.241	0.628	–
	–	–	N : P	1.090	1.532	0.228	–
	Temperature	$p\text{CO}_2$	–	34.35	48.13	**< 0.001***	Lower when temperature is 21°C and $p\text{CO}_2$ is 1000
	Temperature	–	N : P	0.030	0.038	0.847	–

(Continues)

Table 1. Continued

Variable	Factor 1	Factor 2	Factor 3	MS	F	p Value	Effect indicated by Tukey's post hoc test
	–	pCO_2	N : P	0.520	0.728	0.402	–
	Temperature	pCO_2	N : P	0.260	0.369	0.549	–
Photochemical efficiency	Temperature	–	–	0.002	0.124	0.728	–
	–	pCO_2	–	0.048	3.370	0.079	–
	–	–	N : P	0.001	0.083	0.775	–
	Temperature	pCO_2	–	0.001	0.090	0.767	–
	Temperature	–	N : P	0.033	2.309	0.142	–
	–	pCO_2	N : P	0.004	0.298	0.590	–
	Temperature	pCO_2	N : P	0.012	0.832	0.371	–
Maximum electron transport rate	Temperature	–	–	0.050	4.885	**0.037***	Higher at 21°C
	–	pCO_2	–	0.018	1.785	0.194	–
	–	–	N : P	0.001	0.153	0.699	–
	Temperature	pCO_2	–	0.014	1.321	0.262	–
	Temperature	–	N : P	0.235	2.273	0.145	–
	–	pCO_2	N : P	0.001	0.801	0.379	–
	Temperature	pCO_2	N : P	0.134	1.294	0.266	–
Light saturation point	Temperature	–	–	2463	14.03	**< 0.001***	Higher at 21°C
	–	pCO_2	–	311.1	1.772	0.196	–
	–	–	N : P	1.200	0.007	0.937	–
	Temperature	pCO_2	–	565.7	3.222	0.852	–
	Temperature	–	N : P	34.40	0.196	0.662	–
	–	pCO_2	N : P	7.500	0.430	0.838	–
	Temperature	pCO_2	N : P	5.600	0.032	0.859	–
Chlorophyll *a*	Temperature	–	–	0.001	2.115	0.159	–
	–	pCO_2	–	0.001	0.380	0.543	–
	–	–	N : P	0.001	0.386	0.540	–
	Temperature	pCO_2	–	0.001	0.887	0.356	–
	Temperature	–	N : P	0.001	1.207	0.283	–
	–	pCO_2	N : P	0.001	1.814	0.191	–
	Temperature	pCO_2	N : P	0.001	1.006	0.326	–
Integrated biomarker response	Temperature	–	–	3.295	19.41	**< 0.001***	Higher at 21°C
	–	pCO_2	–	0.051	0.301	0.591	–
	–	–	N : P	0.181	1.068	0.317	–
	Temperature	pCO_2	–	0.004	0.026	0.875	–
	Temperature	–	N : P	0.046	0.272	0.609	–
	–	pCO_2	N : P	0.191	1.126	0.304	–
	Temperature	pCO_2	N : P	0.139	0.820	0.378	–
AOX : Resp	Temperature	–	–	0.234	15.97	**< 0.001***	Higher at 21°C
	–	pCO_2	–	0.001	0.024	0.879	–
	–	–	N : P	0.028	1.883	0.183	–
	Temperature	pCO_2	–	0.053	3.621	0.069	–
	Temperature	–	N : P	0.009	0.600	0.446	–
	–	pCO_2	N : P	0.001	0.089	0.768	–
	Temperature	pCO_2	N : P	0.106	7.357	**0.012***	No significant increase when N : P is 16 and pCO_2 is 400
PPC : PSP	Temperature	–	–	0.012	208.3	**< 0.001***	Lower at 21°C
	–	pCO_2	–	0.001	0.865	0.362	–
	–	–	N : P	0.001	0.630	0.435	–

(Continues)

Table 1. Continued

Variable	Factor 1	Factor 2	Factor 3	MS	F	p Value	Effect indicated by Tukey's post hoc test
	Temperature	$p\mathrm{CO}_2$	–	0.001	0.845	0.367	–
	Temperature	–	N : P	0.001	0.067	0.798	–
	–	$p\mathrm{CO}_2$	N : P	0.001	0.309	0.583	–
	Temperature	$p\mathrm{CO}_2$	N : P	0.001	0.749	0.395	–

*Highlights significant *p* values (< 0.05).

determined following Bradford ([1976](#)) to report enzymatic activity in activity unit (U) mg protein^{-1}. To obtain comparable data, all measurements were conducted by a spectrophotometer (Multiskan® Spectrum; Thermo Fisher Scientific) at room temperature (20°C). Activities of antioxidant enzymes and MDA contents are shown in a star plot and were analyzed using the integrated biomarker response (IBR) method suggested by Beliaeff and Burgeot ([2002](#)), which merges the results into one index. The IBR method allows clear visualization (using radar plots and one index) of the biological effects of treatments and simplifies the interpretation as all data is normalized to the same scale with arbitrary units. The IBR only simplifies the data analysis and indicates changes in antioxidant response. A high IBR value can undercover negative or positive changes, that is, great antioxidant defense or oxidative stress, which become clear by looking at the corresponding radar plots. Individual results of antioxidant enzymatic activity and MDA concentration are shown in Supporting Information Figs. S5, S6. Details concerning the calculation of the IBR are available in Beliaeff and Burgeot ([2002](#)).

Samples for Chl *a* and photosynthetic pigments (PSPs) were taken by filtering 250 mL of the culture onto a polycarbonate filter (0.45-μm pore size; Millipore) protected from direct irradiance. The filter was conserved in 2 mL of 100% acetone at −80°C until analysis. Pigments were extracted and subsequently analyzed by high-performance liquid chromatography (Waters Alliance 2695; Agilent), following methods described in Wiltshire et al. ([2000](#)). Pigments quantified in the analysis were Chl *a*, fucoxanthin, diadinoxanthin, β-carotene and violaxanthin. Pigments were divided into "PSPs" (including Chl *a* and fucoxanthin), and "photoprotective carotenoids" (PPC; including diadinoxanthin, violaxanthin, and β-carotene). Individual results of carotenoid contents are shown in Supporting Information Fig. S7.

Statistical analyses

Statistical analyses were performed using R 3.4.3 software (R Core Team [2022](#)). For all analyses, the threshold of significance was set to 0.05. Effects of different temperatures, $p\mathrm{CO}_2$ and N : P were assessed through a three-way ANOVA (three-way ANOVA) followed by a pairwise Tukey post hoc test. Data was log-transformed when normality and homoscedasticity of residuals were not met. All results of the three-way ANOVAs

are presented in Table [1](#). Principal component analysis (PCA) was applied to assess multivariate response to the experimental treatments on the dependent variables using temperature, $p\mathrm{CO}_2$ and N : P ratio as supplementary variables.

Results

Carbon fluxes and cellular carbon content

Primary production, which represents the major share of organic carbon flow into the cell, was significantly affected by temperature as well as by $p\mathrm{CO}_2$, but not by N : P ratios, or by any of the driver combinations. The primary production of *P. tricornutum* was 2.06 pmol C cell^{-1} d^{-1} at 18°C and was higher at 21°C (2.38 pmol C cell^{-1} d^{-1}, $F_{1,24}$ 9.918, $p = 0.004$; Fig. [1](#); Table [1](#)). Primary production was also higher at 1000 μatm $p\mathrm{CO}_2$ than at 400 μatm $p\mathrm{CO}_2$ (2.33 vs. 2.11 pmol C cell^{-1} d^{-1}, $F_{1,24}$ 4.854, $p = 0.037$; Table [1](#)). The dark
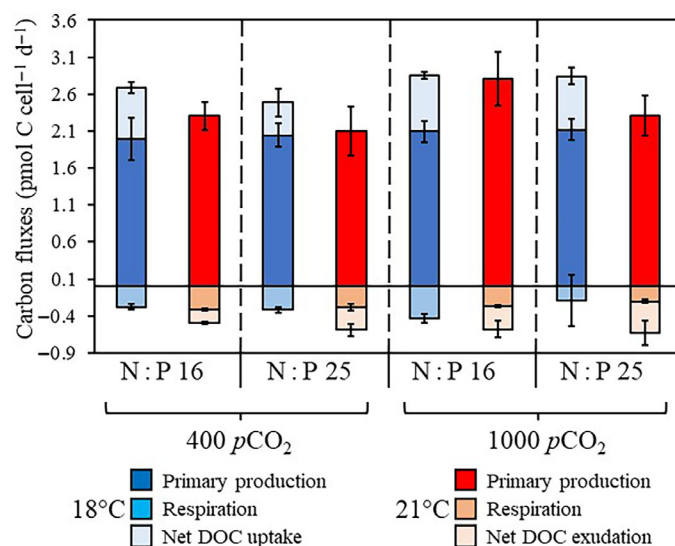
Fig. 1. Carbon fluxes in the *Phaeodactylum tricornutum* cell under different treatments. Carbon production (primary production) and carbon consumption (net DOC production and dark respiration). Positive DOC production represents DOC uptake by the cell, while negative DOC production represents DOC exudation by the cell. The *X*-axis represents N : P ratios and $p\mathrm{CO}_2$. Colors represent temperature (blue = 18°C, red = 21°C). Different shades represent primary production, respiration, and net DOC production. Data as mean ± standard deviation, $n = 4$.
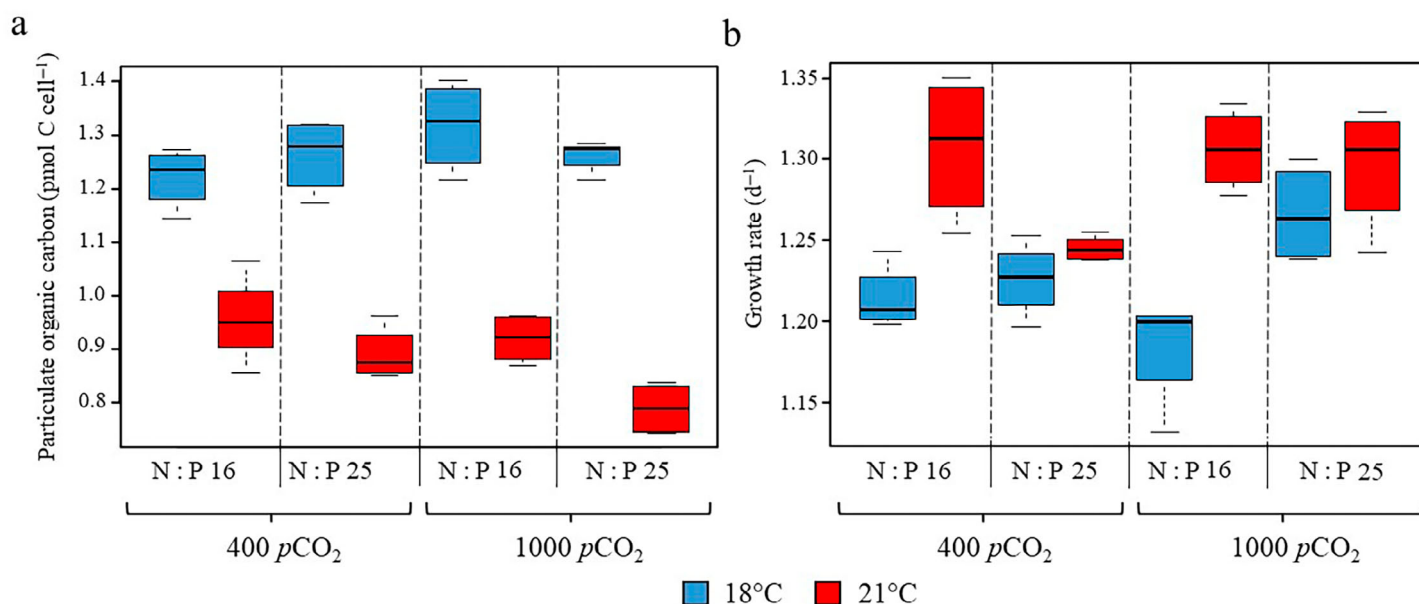
Fig. 2. Cellular carbon content and *Phaeodactylum tricornutum*-specific growth rate. (**a**) Particulate organic matter. (**b**) *P. tricornutum* specific growth rate. The *X*-axis represents N : P ratios and pCO_2. Colors represent temperature (blue = 18°C, red = 21°C), $n = 4$.

respiration rate did not differ between temperatures at pCO_2 of 400 μatm, but it was negatively affected by higher temperatures when pCO_2 was 1000 μatm ($F_{1,24}$ 30.86, $p < 0.001$; Fig. 1; Table 1). Dark respiration rates were unaffected by dissolved N : P ratios. Concerning DOC production, under 21°C, we observed a significant increase for 1000 pCO_2 compared to 400 pCO_2, independent of N : P ratio (0.36 vs. 0.25 pmol cell^{-1} d^{-1}, $F_{1,24}$ 9.542, $p = 0.005$; Fig. 1, Table 1). In addition, DOC production was also significantly stimulated at higher N : P ratios, about 0.13 pmol cell^{-1} d^{-1} on average, independent of temperature and pCO_2 ($F_{1,24}$ 7.023, $p = 0.014$; Table 1). In all 21°C treatments, we observed DOC exudation rates of 0.31 pmol C cell^{-1} d^{-1} on average, independent from N : P and pCO_2, while under 18°C, we found DOC uptake, with rates of 0.65 pmol C cell^{-1} d^{-1}, independent from N : P and pCO_2 ($F_{1,24}$ 400.2, $p < 0.001$; Table 1). Cellular carbon contents were significantly influenced by temperature, being higher at 18°C than at 21°C (1.26 vs. 0.89 pmol C cell^{-1}, $F_{1,24}$ 272.8, $p < 0.001$; Fig. 2a).

Growth rate

Growth rates of *P. tricornutum* were positively affected by higher temperature at 400 μatm pCO_2, but the increase was lower at 1000 μatm pCO_2 ($F_{1,24}$ 15.39, $p < 0.001$; Fig. 2b; Table 1). Furthermore, pCO_2 and N : P ratios in isolation did not significantly influence growth rates, but in combination, a significantly higher growth rate was achieved under 1000 μatm pCO_2 and an N : P of 25, thereby indicating an interactive effect of these drivers. The interaction of temperature and N : P ratios, as well as interactions of all three drivers simultaneously, did not show significant statistical results on growth rates.

Photochemical performance and Chl *a* content

Photochemical efficiency (α) was 0.016 on average in all treatments, and was neither affected by temperature, nor by pCO_2 or N : P ratio ($p > 0.05$; Tables 1, 2). The compensation point (cp) was significantly lower under 21°C and high pCO_2 (10.49 vs. 6.51 μmol photons m^{-2} s^{-1}), but no temperature effect could be detected under low pCO_2, showing the interactivity of these drivers ($F_{1,24}$ 48.31, $p < 0.001$; Tables 1, 2). Maximum rates of net photosynthesis (V_{max}) were positively affected by higher temperature ($F_{1,24}$ 4.885, $p = 0.037$; Table 1), increasing from 1.25 to 1.46 μmol O$_2$ μg Chl a^{-1} h^{-1}. No effects of pCO_2 and N : P were detected. The light saturation point (I_k) was higher under high temperature ($\sim$ 85 vs. $\sim$ 100 μmol photons m^{-2} s^{-1}, $F_{1,24}$ 14.03, $p < 0.001$, Tables 1, 2), irrespective of the applied pCO_2 levels and N : P ratios. None of the above-mentioned photochemical parameters was affected by N : P ratio ($p > 0.05$, Tables 1, 2). Chl *a* content was, on average, 0.15 pg cell^{-1} and was not affected by temperature, pCO_2 or N : P ratio ($p > 0.05$; Tables 1, 2). Table 2 presents the RLC-fitted parameters under different treatments. Apparent photochemical efficiency (α), light compensation point (cp), maximum electron transport rate (V_{max}), light saturation point (I_k) based on the rates of μmol O$_2$ μg Chl a^{-1} h^{-1}. Chl *a* content as pg cell^{-1}. Data as mean $\pm$ standard deviation, $n = 4$.

Antioxidant response

The IBR index was, on average, 4.48 under 18°C, but it was lower at 21°C (0.61, $F_{1,16}$ 19.41, $p < 0.001$; Fig. 3a,b; Table 1), showing that temperature is the main driver for antioxidant responses. We observed no statistically significant effect of pCO_2, dissolved N : P ratios, nor of any driver combination on

Table 2. The rapid light curve fitted parameters under different treatments. Apparent photochemical efficiency (α), light compensation point (cp), maximum electron transport rate (V_{max}), light saturation point (I_k) based on the rates of μmol O_2 μg Chl a^{-1} h^{-1}. Chl a content as pg cell^{-1}. Data as mean $\pm$ standard deviation, $n = 4$.

| | 18°C | | | | 21°C | | | |
| | 400 pCO_2 | | 1000 pCO_2 | | 400 pCO_2 | | 1000 pCO_2 | |
Variable	N : P 16	N : P 25	N : P 16	N : P 25	N : P 16	N : P 25	N : P 16	N : P 25
α	0.015 (±0.003)	0.015 (±0.005)	0.016 (±0.003)	0.020 (±0.004)	0.015 (±0.003)	0.014 (±0.004)	0.019 (±0.004)	0.015 (±0.003)
cp (μmol photons m^{-2} s^{-1})	8.20 (±1.07)	8.21 (±0.28)	10.86 (±0.93)	9.99 (±0.73)	8.41 (±0.28)	8.17 (±0.93)	6.55 (±0.69)	6.17 (±0.49)
V_{max} (μmol O_2 μg Chl a^{-1} h^{-1})	1.14 (±0.18)	1.09 (±0.35)	1.18 (±0.19)	1.57 (±0.43)	1.55 (±0.21)	1.38 (±0.37)	1.59 (±0.09)	1.33 (±0.12)
I_k (μmol photons m^{-2} s^{-1})	86.3 (±6.2)	82.1 (±1.7)	86.7 (±3.1)	86.1 (±8.1)	109.4 (±9.8)	110.9 (±20.4)	94.6 (±17.1)	96.4 (±11.5)
Chl a content (pg cell^{-1})	0.15 (±0.01)	0.15 (±0.03)	0.15 (±0.02)	0.12 (±0.02)	0.15 (±0.01)	0.16 (±0.03)	0.15 (±0.01)	0.16 (±0.01)

the IBR. The temperature-driven decrease in IBR was mainly caused by the lower activity of antioxidant enzymes, especially GPx, GST, and SOD-Mn (Fig. 3a,b; Supporting Information Fig. S5). Cellular MDA concentrations were stimulated by temperature in all treatments ($F_{1,16}$ 18.06, $p < 0.001$; Table 1). In all 18°C treatments, MDA concentrations were highest under high pCO_2 and high N : P (Fig. 3a). The ratio of AOX to dark respiration was significantly stimulated by high temperatures in all driver constellations, going from 0.20 to 0.40, except under low pCO_2 and low N : P (Fig. 4a). The ratio of PPCs (violaxanthin, diadinoxanthin, β-carotene) to PSPs (Chl a, fucoxanthin; PPC : PSP) decreased under high temperatures in all treatments ($F_{1,24}$ 208.3, $p < 0.001$; Fig. 4b; Table 1). Since PSPs were not different across treatments, the reduction of this ratio was primarily driven by the decrease in PPCs (Supporting Information Fig. S7; Tables 1, 2).

Synthesis of cellular responses

Results from the PCA identified temperature as the most influential driver of changes in the measured variables, followed by pCO_2 and, to a lower degree, N : P ratio (Fig. 5). The first two principal component axes of the PCA explained 60.2% of variance within all observations (Fig. 5). Higher DOC production, growth rate, and MDA concentration were related to higher temperature (21°C), whilst higher POC, dark respiration rate, and antioxidant response were positively correlated to the lower temperature we tested (18°C). On the other hand, primary production and maximum net photosynthesis rates (V_{max}) were rather influenced by pCO_2 than by temperature, whereas contents of PSPs, Chl a and fucoxanthin, were the least influenced by the environmental drivers.

Discussion

The full-factorial design of our experiment enabled us to identify that in the global change context tested in this study, temperature has a greater influence than higher pCO_2 and dissolved N : P ratios on the antioxidant capacity and carbon metabolism of *P. tricornutum*. Higher temperatures led to higher photosynthesis, DOC exudation, growth rate and respiration, overall yielding a decrease in net C fluxes into the cell, and cells with lower carbon content. We also observed a synergy between temperature and pCO_2, and, to a lesser extent, between temperature and N : P. The cells were mostly unaffected by pCO_2 and N : P ratio at 18°C, and only under increased temperatures, cells became prone to these environmental drivers. At 21°C, the phytoplankton cells had higher oxidative stress and lower antioxidant enzymatic activity, indicating a reduced capacity to combat ROS generated under warmer conditions. These results indicate that the RCP 8.5 scenario predicted for 2100 may influence the carbon metabolism and oxidative stress management of phytoplankton with implications for oceanic carbon fluxes. A decrease in cellular carbon content and increase of DOC production might
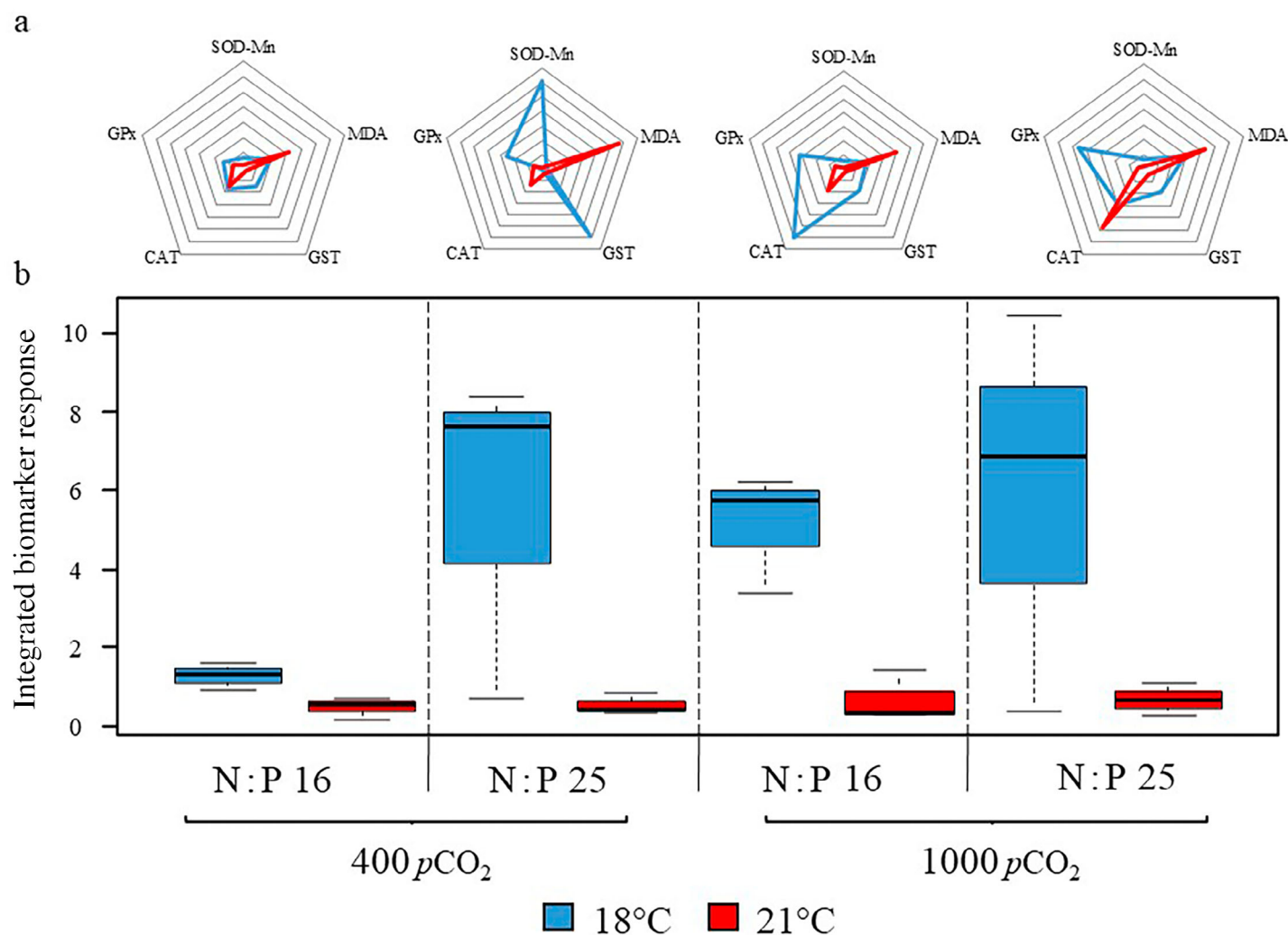
Fig. 3. Antioxidant enzymatic response and oxidative stress. (**a**) Normalized radar plots of antioxidant enzyme activities and MDA as a biomarker for oxidative stress. MDA = malondialdehyde, SOD-Mn = manganese superoxide dismutase, GST = glutathione *S*-transferase, CAT = catalase, GPx = glutathione peroxidase. All radar plots are to the same scale. (**b**) Integrated biomarker response. The *X*-axis represents N : P ratios and pCO_2. Colors represent temperature (blue = 18°C, red = 21°C), $n = 3$.

represent a higher carbon input into the surface microbial loop and less export of organic matter to deeper waters, since carbon fixed as biomass can be assimilated to higher trophic levels, while DOC is usually a source of energy for planktonic bacteria (Azam et al. 1983).

We observed higher cellular contents of MDA, and a higher electron flow through the AOX pathway under 21°C than at 18°C. Both are indicators of oxidative stress, because the cells reroute electrons through the AOX pathway to alleviate flow through the inner mitochondrial membrane, and because MDA arises from harmful oxidation reactions in lipid membranes (Uchiyama and Mihara 1978). The chloroplast and mitochondrion constantly exchange compounds such as ADP/ATP and electron carriers, whereby the mitochondrion can serve as an extra electron sink under photosynthetic

overproduction by activating the AOX pathway. This generates less energy, but allows a more rapid supply of ADP and electron carriers to the chloroplast, avoiding photoinhibition due to the lack of these compounds in the chloroplast (Bailleul et al. 2015; Launay et al. 2020). The increase of AOX : Respiration we observed under elevated temperature, despite lower dark respiration and higher photosynthetic rates, suggests that the mitochondrion was acting as an electron sink as a stress response mechanism (Allen et al. 2008; Prihoda et al. 2012). Regarding the detoxification of oxidative stress, we observed an overall lower activity of most antioxidant enzymes under high temperatures (GPx, GST, SOD-Mn; CAT under low N : P). This is counterintuitive, since higher temperatures should increase molecular movements and thus, enhance enzymes activity. However, these results are
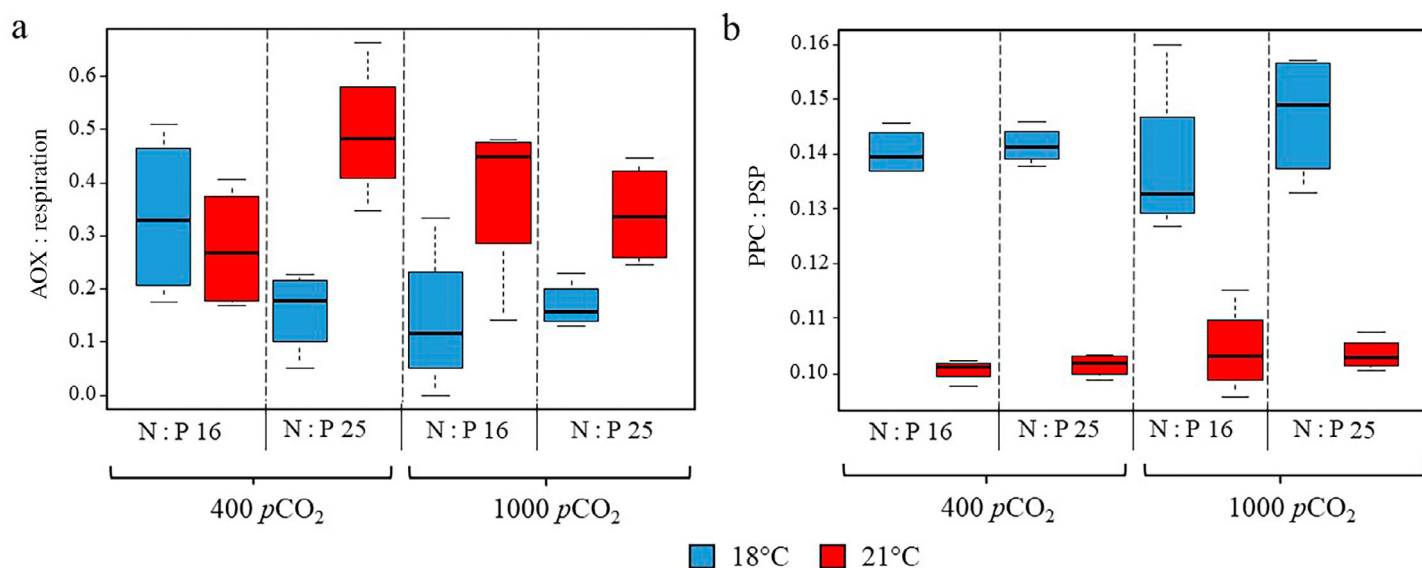
Fig. 4. Alternative oxidase activity and carotenoids. (**a**) Ratio of alternative oxidase (AOX) activity relative to dark respiration rate. (**b**) Ratio of photoprotective carotenoids (PPC, diadinoxanthin, violaxanthin, and β-carotene) relative to photosynthetic pigments (PSP, chlorophyll *a* and fucoxanthin). The *X*-axis represents N : P ratios and pCO_2. Colors represent temperature (blue = 18°C, red = 21°C), $n = 4$.

supported by another study which also observed decreased activities of antioxidant enzymes in phytoplankton after high-temperature acclimation (Perelman et al. 2006). We hypothesize that these lower enzyme activities reflect the inability of the mitochondria to maintain the respective gene expression, suggesting that 21°C is the supraoptimal temperature for *P. tricornutum*, similar as in other studies (Bitaubé Pérez et al. 2008; He et al. 2014; Tong et al. 2021).

We observed a higher photosynthetic rate at 21°C than at 18°C, which may originate from a thermal enhancement of electron flow in photosynthetic light reaction, and/or from an enhanced activity of the CO_2 fixing enzyme RuBisCo under higher temperatures (Table 2; Ras et al. 2013). In addition to warming, elevated pCO_2 further increased photosynthetic activity, likely as a result of higher C availability, which may enable a reallocation of energy, possibly due to lower demand for the carbon concentration mechanism activity (Young et al. 2015; Rokitta et al. 2022). Light-harvesting pigments (Chl *a*, fucoxanthin) were not affected by any of the drivers, indicating that the light-harvesting portion of the antenna complex was not affected by temperature, pCO_2, or dissolved nutrient ratios. However, the concentration of protective carotenoids (especially diadinoxanthin and violaxanthin; Arbones et al. 2000; Wagner et al. 2006; Janknegt et al. 2008) and their precursor, β-carotene (Kuczynska et al. 2015), decreased under high temperature. This likely enhanced the overall photosynthetic activity, because relatively more captured photons were directed to the light-dependent reactions of photosynthesis. Protective carotenoids compete for light energy trapping in the photosystem and dissipate it as thermal energy before it reaches the reaction center, a useful photoprotection mechanism when light irradiance is higher than needed (Arbones et al. 2000; Wagner et al. 2006; Janknegt et al. 2008). On the one hand, the lower concentration of carotenoids can increase photosynthetic rates, on the other hand, this reduction decreases photoprotection, the main short-term response against the formation of ROS in the chloroplast (Kuczynska et al. 2015). These results, then, suggest that photosynthesis was not a major source of ROS under the tested conditions.

High pCO_2 increased the photosynthetic compensation points (Table 2), meaning that cells needed more light to reach positive net primary production, at 18°C, whereas at 21°C, high pCO_2 lowered the photosynthetic compensation point. Although elevated pCO_2 represents a higher availability of DIC for phytoplankton and could stimulate their growth (Riebesell et al. 2007), it also represents a higher [H^+] concentration. This lowers seawater pH, which influences the membrane potential, intracellular pH, activity of enzymes, and energy partitioning (Riebesell 2004; Giordano et al. 2005; Rokitta et al. 2012), and can even lead to lower growth rates (Berge et al. 2010), counterbalancing the positive effect of DIC fertilization. We hypothesize that the overall mitochondrial function was negatively affected by increasing temperature, which was exacerbated under high pCO_2. In other words, respiration had the opposite reaction to temperature and pCO_2 as photosynthesis. This is unexpected since, typically, dark respiration is positively correlated with photosynthesis, acting as a sink for organic carbon (Yoshida et al. 2007), and also for the reduction equivalents (Bailleul et al. 2015). This disparity of chloroplast and mitochondrial activity reveals an imbalance under high temperature, which has been observed previously
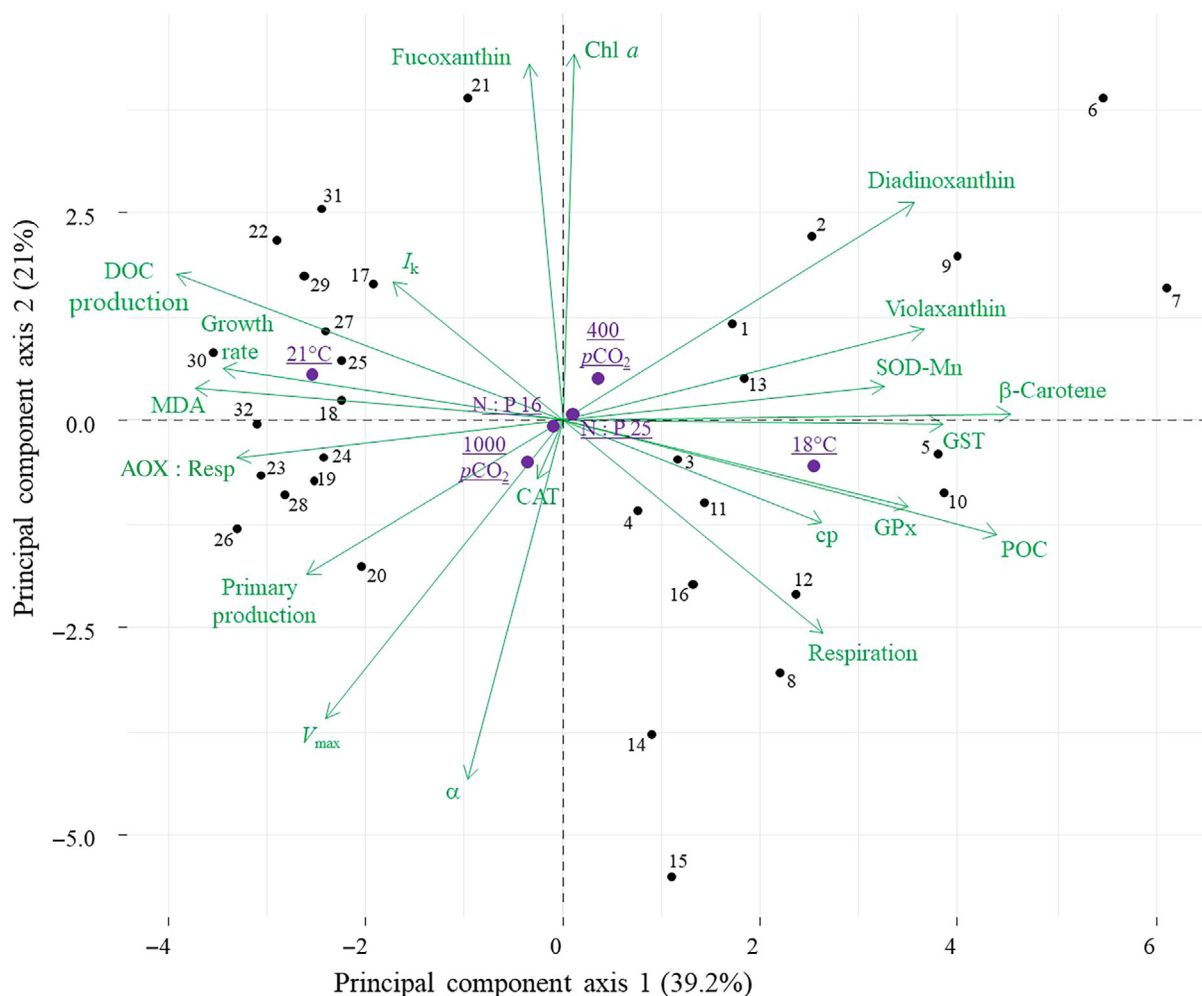
Fig. 5. Principal component analysis (PCA) of the *Phaeodactylum tricornutum* response to climate change factors. Dependent variables are displayed in green, supplementary variables are displayed in purple and black dots represent the individual observations (replicates). The two first principal component axes explain 60.2% of all variation within observations. Location of dependent variables near to supplementary variables indicates positive correlation of that experimental factor on the dependent variable. The position of the supplementary variables (drivers) relative to the point 0 show the intensity of the drivers on the dependent variables. The further the drivers are from point 0, the stronger their effect is. Black dots represent individual replicates: 1–4 (T: 18°C, pCO$_2$ 400 μatm, N : P 16), 5–8 (T: 18°C, pCO$_2$ 400 μatm, N : P 25), 9–12 (T: 18°C, pCO$_2$ 1000 μatm, N : P 16), 12–16 (T: 18°C, pCO$_2$ 1000 μatm, N : P 25), 17–20 (T: 21°C, pCO$_2$ 400 μatm, N : P 16), 21–24 (T: 21°C, pCO$_2$ 400 μatm, N : P 25), 25–28 (T: 21°C, pCO$_2$ 1000 μatm, N : P 16), and 29–32 (T: 21°C, pCO$_2$ 1000 μatm, N : P 25).

in this species, for instance, by Tong et al. (2021), who found that respiration peaked at 18°C while photosynthesis had an optimum around 20°C. The negative effect of high pCO$_2$ on dark respiration has also been observed in diatoms before (Shi et al. 2019). This imbalance causes high photosynthetic organic carbon production, as well as reduced respiration, which should lead to higher organic carbon retention, that is, both processes should support the net POC production of the cells. However, phytoplankton cells did not accumulate POC, but rather, we observed an increased DOC exudation (especially under a high N : P ratio), which may represent a mechanism to regulate cellular POC production rates. DOC exudation has previously been shown to range from 1% to 55% of the total carbon fixation in different phytoplankton

taxa. In line with our data, DOC production was found to be stimulated by high temperatures, as well as by higher pCO$_2$ (Zlotnik and Dubinsky 1989; Baines and Pace 1991; Riebesell et al. 2007; Wetz and Wheeler 2007; Engel et al. 2010; Torstensson et al. 2015). The stimulating effect of high N : P ratios on DOC production has been found before in phytoplankton (Li and Sun 2016), and seems to be an additional supporting mechanism to balance cellular elemental stoichiometry (Thornton 2014), since RuBisCO activity is more sensitive to low supplies of nitrogen than of phosphorus (Geider et al. 1993). It is important to note that, throughout the experiment, cells had a replete supply of nutrients, meaning that the effects of nutrients seen here are solely assigned to the ratios of N : P ratio. Effects of higher N : P ratios might

have been even more pronounced when cells experience nutrient limitation. Although, *P. tricornutum* and other phytoplankton species can take up DOC (Villanova et al. 2017), the net cellular flows of DOC were sensitive to the environmental drivers tested here. We measured DOC uptake at 18°C and exudation at 21°C, with a synergistic influence of warming, elevated pCO_2, and elevated N : P ratios on the degree of DOC exudation. These results are supported by another study, which found higher DOC exudation by phytoplankton under oxidative stress as well (Mohamed 2008). While the stimulated photosynthetic POC production and the lower consumption by mitochondrial respiration under high temperature were compensated by DOC exudation, other temperature effects could not be compensated, for instance, the stimulation of growth rates that typically derive from enhanced nutrient uptake, more rapid DNA duplication, and so forth. Consequently, given the steady net POC production, the increased division rates resulted in cells with overall lower carbon content. Our study shows that, while warmer temperatures stimulate the growth rate of the phytoplankton *P. tricornutum*, there are significant tradeoffs between growth and other metabolic processes in the cell. At higher growth rates, we found evidence of oxidative stress, deviating route via the AOX pathway and higher DOC exudation.

If the results obtained for this single strain of one species are indicative of what would happen with other species as well, an expected scenario for 2100 corresponding to RCP 8.5 with higher temperature and pCO_2 combined with increasing N : P ratio might significantly alter metabolic fluxes of microalgae and have the potential to alter the biogeochemical cycling of carbon in the oceans. An increased photosynthesis, as well as a decreased respiration might lower the overall CO_2 concentrations in surface waters and could enhance air-sea gas exchange, that is, the uptake of atmospheric CO_2. The fact that organic carbon is not channeled into biomass and fed to higher trophic levels, but rather exuded, suggests an enhanced carbon input into the microbial loop (Azam et al. 1983). In line with this, cells with lower C content might be smaller and likely to have lower sinking velocities and also to become better prey, especially for microzooplankton, which again will feed more carbon into the microbial loop (Legendre and Le Fèvre 1995; Morán et al. 2010; Hillebrand et al. 2022). Similar results were obtained in a mesocosm experiment during which plankton communities were subjected to simultaneous changes in temperature, pCO_2, and N : P ratios (Moreno et al. 2022), and which identified an intensification of the microbial loop. Evidence have been also found that higher DOC availability (Hitchcock et al. 2010) and warming (Hoppe et al. 2002, 2008) lead to a higher abundance of bacterioplankton. Nevertheless, clearer effects on bacteria abundance might be seen after phytoplankton reach the stationary phase and nutrient depletion, when bacteria abundance increases considerably (Moreno et al. 2022). These results highlight the sensitivity of microalgal physiology to the combined effects of multiple drivers. Remarkably, the manifestation of further effects of pCO_2 and N : P were enabled by elevated temperatures, underlining that temperature functions as a "master variable" for phototrophic phytoplankton. An enhanced oceanic CO_2 uptake and an overall stimulated microbial loop may be the longer-term consequences of rising temperatures, elevated pCO_2 as well as shifted dissolved N : P ratios.

Data availability statement

The data that support the findings of this study are openly available in the PANGAEA platform at https://doi.org/10.1594/PANGAEA.947112.

References

Aebi, H. 1984. Catalase in vitro, p. 121–126. *In* L. Packer [ed.], Methods in enzymology, v. **105**. Academic Press/Elsevier. doi:10.1016/S0076-6879(84)05016-3

Ahmad, S., and R. S. Pardini. 1988. Evidence for the presence of glutathione peroxidase activity towards an organic hydroperoxide in larvae of the cabbage looper moth, *Trichoplusia ni*. Insect Biochem. **18**: 861–866. doi:10.1016/0020-1790(88)90111-4

Alipanah, L., J. Rohloff, P. Winge, A. M. Bones, and T. Brembu. 2015. Whole-cell response to nitrogen deprivation in the diatom *Phaeodactylum tricornutum*. J. Exp. Bot. **66**: 6281–6296. doi:10.1093/jxb/erv340

Allen, A. E., and others. 2008. Whole-cell response of the pennate diatom *Phaeodactylum tricornutum* to iron starvation. Proc. Natl. Acad. Sci. USA **105**: 10438–10443. doi:10.1073/pnas.0711370105

Allesson, L., L. Ström, and M. Berggren. 2016. Impact of photochemical processing of DOC on the bacterioplankton respiratory quotient in aquatic ecosystems. Geophys. Res. Lett. **43**: 7538–7545. doi:10.1002/2016GL069621

Alvarez-Fernandez, S., L. T. Bach, J. Taucher, U. Riebesell, U. Sommer, N. Aberle, C. P. D. Brussaard, and M. Boersma. 2018. Plankton responses to ocean acidification. The role of nutrient limitation. Prog. Oceanogr. **165**: 11–18. doi:10.1016/j.pocean.2018.04.006

Anderson, T. R., E. Hawkins, and P. D. Jones. 2016. CO_2, the greenhouse effect and global warming: From the pioneering work of Arrhenius and Callendar to today's earth system models. Endeavour **40**: 178–187. doi:10.1016/j.endeavour.2016.07.002

Arbones, B., F. G. Figueiras, and R. Varela. 2000. Action spectrum and maximum quantum yield of carbon fixation in natural phytoplankton populations: Implications for primary production estimates in the ocean. J. Mar. Syst. **26**: 97–114. doi:10.1016/S0924-7963(00)00042-7

Azam, F., T. Fenchel, J. G. Field, J. S. Gray, L. A. Meyer-Reil, and F. Thingstad. 1983. The ecological role of water-

column microbes in the sea. Mar. Ecol. Prog. Ser. **10**: 257–263. doi:10.3354/meps010257

Bach, L. T., N. Hernández-Hernández, J. Taucher, C. Spisla, C. Sforna, U. Riebesell, and J. Arístegui. 2019. Effects of elevated CO_2 on a natural diatom community in the subtropical NE Atlantic. Front. Mar. Sci. **6**: 75. doi:10.3389/fmars.2019.00075

Bailleul, B., and others. 2015. Energetic coupling between plastids and mitochondria drives CO_2 assimilation in diatoms. Nature **524**: 366–369. doi:10.1038/nature14599

Baines, S. B., and M. L. Pace. 1991. The production of dissolved organic matter by phytoplankton and its importance to bacteria: Patterns across marine and freshwater systems. Limnol. Oceanogr. **36**: 1078–1090. doi:10.4319/lo.1991.36.6.1078

Barros, M. P., M. Pedersén, P. Colepicolo, and P. Snoeijs. 2003. Self-shading protects phytoplankton communities against H_2O_2-induced oxidative damage. Aquat. Microb. Ecol. **30**: 275–282. doi:10.3354/ame030275

Beardall, J., and J. A. Raven. 2004. The potential effects of global climate change on microalgal photosynthesis, growth and ecology. Phycologia **43**: 26–40. doi:10.2216/i0031-8884-43-1-26.1

Beliaeff, B., and T. Burgeot. 2002. Integrated biomarker response: A useful tool ecological risk. Environ. Toxicol. Chem. **21**: 1316–1322. doi:10.1002/etc.5620210629

Berge, T., N. Daugbjerg, B. B. Andersen, and P. J. Hansen. 2010. Effect of lowered pH on marine phytoplankton growth rates. Mar. Ecol. Prog. Ser. **416**: 79–91. doi:10.3354/meps08780

Berges, J. A., D. J. Franklin, and P. J. Harrison. 2001. Evolution of an artificial seawater medium: Improvements in enriched seawater, artificial water over the last two decades. J. Phycol. **37**: 1138–1145. doi:10.1046/j.1529-8817.2001.01052.x

Bitaubé Pérez, E., I. C. Pina, and L. Pérez Rodríguez. 2008. Kinetic model of growth of *Phaeodactylum tricornutum* in intensive culture photobioreactor. Biochem. Eng. J. **40**: 520–525. doi:10.1016/j.bej.2008.02.007

Bowler, C., and others. 2008. The *Phaeodactylum* genome reveals the evolutionary history of diatom genomes. Nature **456**: 239–244. doi:10.1038/nature07410

Bowler, C., A. Vardi, and A. E. Allen. 2010. Oceanographic and biogeochemical insights from diatom genomes. Ann. Rev. Mar. Sci. **2**: 333–365. doi:10.1146/annurev-marine-120308-081051

Bradford, M. M. 1976. A rapid and sensitive method for the quantitation of microgram quantities of protein utilizing the principle of protein-dye binding. Anal. Biochem. **72**: 248–254. doi:10.1006/abio.1976.9999

Brutemark, A., J. Engström-Öst, A. Vehmaa, and E. Gorokhova. 2015. Growth, toxicity and oxidative stress of a cultured cyanobacterium (*Dolichospermum* sp.) under different CO_2/pH and temperature conditions. Phycol. Res. **63**: 56–63. doi:10.1111/pre.12075

Buesseler, K. O. 1998. The decoupling of production and particulate export in the surface. Global Biogeochem. Cycles **12**: 297–310. doi:10.1029/97GB03366

Choo, K., P. Snoeijs, and M. Pederse. 2004. Oxidative stress tolerance in the filamentous green algae *Cladophora glomerata* and *Enteromorpha ahlneriana*. J. Exp. Mar. Biol. Ecol. **298**: 111–123. doi:10.1016/j.jembe.2003.08.007

Day, D. A., and J. T. Wiskich. 1995. Regulation of alternative oxidase activity in higher plants. J. Bioenerg. Biomembr. **27**: 379–385. doi:10.1007/BF02110000

Dickson, A. G. 1981. An exact definition of total alkalinity and a procedure for the estimation of alkalinity and total inorganic carbon from titration data. Deep-Sea Res. Part I Oceanogr. Res. **28**: 609–623. doi:10.1016/0198-0149(81)90121-7

Dickson, A. G., and F. J. Millero. 1987. A comparison of the equilibrium constants for the dissociation of carbonic acid in seawater media. Deep-Sea Res. I Oceanogr. Res. **34**: 1733–1743. doi:10.1016/0198-0149(87)90021-5

Doney, S. C., V. J. Fabry, R. A. Feely, and K. A. Kleypas. 2009. Ocean acidification: The other CO_2 problem. Ann. Rev. Mar. Sci. **1**: 169–192. doi:10.1146/annurev.marine.010908.163834

Duarte, C. M., and J. Cebrián. 1996. The fate of marine autotrophic production. Limnol. Oceanogr. **41**: 1758–1766. doi:10.4319/lo.1996.41.8.1758

Dubinsky, Z., and N. Stambler. 2009. Photoacclimation processes in phytoplankton: Mechanisms, consequences and applications. Aquat. Microb. Ecol. **56**: 163–176. doi:10.3354/ame01345

Engel, A., N. Händel, J. Wohlers, M. Lunau, H. P. Grossart, U. Sommer, and U. Riebesell. 2010. Effects of sea surface warming on the production and composition of dissolved organic matter during phytoplankton blooms: Results from a mesocosm study. J. Plankton Res. **33**: 357–372. doi:10.1093/plankt/fbq122

Gao, K., and D. A. Campbell. 2014. Photophysiological responses of marine diatoms to elevated CO_2 and decreased pH: A review. Funct. Plant Biol. **41**: 449–459. doi:10.1071/FP13247

Gechev, T. S., F. Van Breusegem, J. M. Stone, I. Denev, and C. Laloi. 2006. Reactive oxygen species as signals that modulate plant stress responses and programmed cell death. Bioessays **28**: 1091–1101. doi:10.1002/bies.20493

Geider, R. J., J. La Roche, R. M. Greene, and M. Olaizola. 1993. Response of the photosynthetic apparatus of *Phaeodactylum tricornutum* (Bacillariophyceae) to nitrate, phosphate, or iron starvation. J. Phycol. **29**: 755–766. doi:10.1111/j.0022-3646.1993.00755.x

Gillespie, K. M., A. Rogers, and E. A. Ainsworth. 2011. Growth at elevated ozone or elevated carbon dioxide concentration alters antioxidant capacity and response to acute oxidative stress in soybean (*Glycine max*). J. Exp. Bot. **62**: 2667–2678. doi:10.1093/jxb/erq435

Giordano, M., J. Beardall, and J. A. Raven. 2005. CO_2 concentrating mechanisms in algae: Mechanisms, environmental modulation, and evolution. Annu. Rev. Plant Biol. **56**: 99–131. doi:10.1146/annurev.arplant.56.032604.144052

Goldman, J. A. L., M. L. Bender, and F. M. M. Morel. 2017. The effects of pH and pCO$_2$ on photosynthesis and respiration in the diatom *Thalassiosira weissflogii*. Photosynth. Res. **132**: 83–93. doi:10.1007/s11120-016-0330-2

Grizzetti, B., F. Bouraoui, and A. Aloe. 2012. Changes of nitrogen and phosphorus loads to European seas. Glob. Change Biol. **18**: 769–782. doi:10.1111/j.1365-2486.2011.02576.x

Guillard, R. R. L. 1975. Culture of phytoplankton for feeding marine invertebrate, p. 296–360. *In* W. L. Smith and M. H. Chanley [eds.], Culture of marine invertebrates animals. Plenum. doi:10.1007/978-1-4615-8714-9_3

Habig, W. H., and W. B. Jakoby. 1981. Glutathione *S*-transferases (rat and human), p. 218–235. *In* W. B. Jakoby [ed.], Methods in enzymology: Detoxication and drug metabolism: Conjugation and related systems, v. **77**. Academic Press/Elsevier. doi:10.1016/S0076-6879(81)77029-0

Halliwell, B. 1987. Oxidative damage, lipid peroxidation and antioxidant protection in chloroplasts. Chem. Phys. Lipids **44**: 327–340. doi:10.1016/0009-3084(87)90056-9

Hancke, K., T. B. Hancke, L. M. Olsen, and G. Johnsen. 2008. Temperature effects on microalgal photosynthesis-light responses measured by O_2 production, pulse-amplitude-modulated fluorescence, and ^{14}C assimilation. J. Phycol. **44**: 501–514. doi:10.1111/j.1529-8817.2008.00487.x

Harrison, P. J., R. E. Waters, and F. J. R. Taylor. (1980). A broad spectrum artificial sea water medium for coastal and open ocean phytoplankton 1. J. Phycol. **16**: 28–35.

He, L., X. Han, and Z. Yu. 2014. A rare *Phaeodactylum tricornutum* cruciform morphotype: Culture conditions, transformation and unique fatty acid characteristics. PloS One **9**: e93922. doi:10.1371/journal.pone.0093922

Hendey, N. I. 1954. Note on the Plymouth *Nitzschia* culture. J. Mar. Biol. Assoc. UK **33**: 335–339. doi:10.1017/S0025315400008377

Hendey, N. I. 1964. An introductory account of the smaller algae of British coastal waters. Part V Bacillariophyceae (Diatoms). Her Majesty's Stationery Office.

Hillebrand, H., E. Acevedo-Trejos, S. D. Moorthi, A. Ryabov, M. Striebel, P. K. Thomas, and M. Schneider. 2022. Cell size as driver and sentinel of phytoplankton community structure and functioning. Funct. Ecol. **36**: 276–293. doi:10.1111/1365-2435.13986

Hitchcock, J. M., S. M. Mitrovic, T. Kobayashi, and D. P. Westhorpe. 2010. Responses of estuarine bacterioplankton, phytoplankton and zooplankton to dissolved organic carbon (DOC) and inorganic nutrient additions. Estuarine Coasts **33**: 78–91. doi:10.1007/s12237-009-9229-x

Honjo, S., and S. J. Manganini. 1993. Annual biogenic particle fluxes to the interior of the North Atlantic Ocean; studied at 34°N 21°W and 48°N 21°W. Deep-Sea Res. II Top. Stud. Oceanogr. **40**: 587–607. doi:10.1016/0967-0645(93)90034-K

Hoppe, H.-G., K. Gocke, R. Koppe, and C. Begler. 2002. Bacterial growth and primary production along a north-south transect of the Atlantic Ocean. Nature **416**: 168–171. doi:10.1038/416168a

Hoppe, H.-G., P. Breithaupt, K. Walther, R. Koppe, S. Bleck, U. Sommer, and K. Jürgens. 2008. Climate warming in the winter affects the coupling between phytoplankton and bacteria during the spring bloom: A mesocosm study. Aquat. Microb. Ecol. **51**: 105–115. doi:10.3354/ame01998

IPCC. 2021. Summary for policymakers. *In* V. Masson-Delmotte and others [eds.], Climate change 2021: The physical science basis. Contribution of working group I to the sixth assessment report of the intergovernmental panel on climate change. Cambridge Univ. Press.

Janknegt, P. J., W. H. Van De Poll, R. J. W. Visser, J. W. Rijstenbil, and A. G. J. Buma. 2008. Oxidative stress response in the marine antarctic diatom *Chaetoceros brevis* (Bacillariophyceae) during photoacclimation. J. Phycol. **44**: 957–966. doi:10.1111/j.1529-8817.2008.00553.x

Jiao, N., and others. 2010. Microbial production of recalcitrant dissolved organic matter: Long-term carbon storage in the global ocean. Nat. Rev. Microbiol. **8**: 593–599. doi:10.1038/nrmicro2386

Kuczynska, P., M. Jemiola-Rzeminska, and K. Strzalka. 2015. Photosynthetic pigments in diatoms. Mar. Drugs **13**: 5847–5881. doi:10.3390/md13095847

Kudo, I., M. Miyamoto, Y. Noiri, and Y. Maita. 2000. Combined effects of temperature and iron on the growth rate and physiology of the marine diatom *Phaeodactylum tricornutum* (Bacillariophyceae). J. Phycol. **36**: 1096–1102. doi:10.1046/j.1529-8817.2000.99042.x

Kvernvik, A. C., S. D. Rokitta, E. Leu, L. Harms, T. M. Gabrielsen, B. Rost, and C. J. Hoppe. 2020. Higher sensitivity towards light stress and ocean acidification in an Arctic Sea-ice-associated diatom compared to a pelagic diatom. New Phytol. **226**: 1708–1724. doi:10.1111/nph.16501

Kvíderová, J., and J. Lukavský. 2003. The cultivation of *Phaeodactylum tricornutum* in crossed gradients of temperature and light. Algolog. Stud. **110**: 67–80. doi:10.1127/1864-1318/2003/0110-0067

Lakeman, M. B., P. von Dassow, and R. A. Cattolico. 2009. The strain concept in phytoplankton ecology. Harmful Algae **8**: 746–758. doi:10.1016/j.hal.2008.11.011

Launay, H., W. Huang, S. C. Maberly, and B. Gontero. 2020. Regulation of carbon metabolism by environmental conditions: A perspective from diatoms and other chromalveolates. Front. Plant Sci. **11**: 1033. doi:10.3389/fpls.2020.01033

Lee, S., and J. A. Fuhrman. 1987. Relationships between biovolume and biomass of naturally derived marine bacterioplankton. Appl. Environ. Microbiol. **53**: 1298–1303. doi:10.1128/aem.53.6.1298-1303.1987

Legendre, L., and J. Le Fèvre. 1995. Microbial food webs and the export of biogenic carbon in oceans. Aquat. Microb. Ecol. **9**: 69–77. doi:10.3354/AME009069

Lesser, M. P. 1997. Oxidative stress causes coral bleaching during exposure to elevated temperatures. Coral Reefs **16**: 187–192. doi:10.1007/s003380050073

Li, J., and X. Sun. 2016. Effects of different phosphorus concentrations and N/P ratios on the growth and photosynthetic characteristics of *Skeletonema costatum* and *Prorocentrum donghaiense*. Chin. J. Oceanol. Limnol. **34**: 1158–1172. doi:10.1007/s00343-016-5169-z

Mallick, N., F. H. Mohn, C. J. Soeder, and J. U. Grobbelaar. 2002. Ameliorative role of nitric oxide on H_2O_2 toxicity to a chlorophycean alga *Scenedesmus obliquus*. J. Gen. Appl. Microbiol. **48**: 1–7. doi:10.2323/jgam.48.1

Marie, D., N. Simon, and D. Vaulot. 2005. Phytoplankton cell counting by flow cytometry, p. 253–267. *In* Algal culturing techniques, v. **1**. Academic Press.

Marra, J., and R. T. Barber. 2004. Phytoplankton and heterotrophic respiration in the surface layer of the ocean. Geophys. Res. Lett. **31**: L09314. doi:10.1029/2004GL019664

Martin-Jézéquel, V., and B. Tesson. 2013. *Phaeodactylum tricornutum* polymorphism: An overview, p. 43–80. *In* K. Heimann and C. Katsaros [eds.], Advances in algal cell biology. Walter De Gruyter Publishing Group. doi:10.1515/9783110229615.43

Mehrbach, C., C. H. Culberson, J. E. Hawley, and R. M. Pytkowicx. 1973. Measurement of the apparent dissociation constants of carbonic acid in seawater at atmospheric pressure. Limnol. Oceanogr. **18**: 897–907. doi:10.4319/lo.1973.18.6.0897

Mittler, R., S. Vanderauwera, M. Gollery, and F. Van Breusegem. 2004. Reactive oxygen gene network of plants. Trends Plant Sci. **9**: 490–498. doi:10.1016/j.tplants.2004.08.009

Mohamed, Z. A. 2008. Polysaccharides as a protective response against microcystin-induced oxidative stress in *Chlorella vulgaris* and *Scenedesmus quadricauda* and their possible significance in the aquatic ecosystem. Ecotoxicology **17**: 504–516. doi:10.1007/s10646-008-0204-2

Morán, X. A. G., A. López-Urrutia, A. Calvo-Díaz, and W. K. W. Li. 2010. Increasing importance of small phytoplankton in a warmer ocean. Glob. Change Biol. **16**: 1137–1144. doi:10.1111/j.1365-2486.2009.01960.x

Moreno, H. D., M. Köring, J. Di Pane, N. Tremblay, K. H. Wiltshire, M. Boersma, and C. L. Meunier. 2022. An integrated multiple driver mesocosm experiment reveals the effect of global change on planktonic food web structure. Commun. Biol. **5**: 179. doi:10.1038/s42003-022-03105-5

Neori, A., and O. Holm-Hansen. 1982. Effect of temperature on rate of photosynthesis in Antarctic phytoplankton. Polar Biol. **1**: 33–38. doi:10.1007/BF00568752

Obernosterer, I., and G. J. Herndl. 1995. Phytoplankton extracellular release and bacterial growth: Dependence on the inorganic N:P ratio. Mar. Ecol. Prog. Ser. **116**: 247–257. doi:10.3354/meps116247

Oudot-Le Secq, M. P., J. Grimwood, H. Shapiro, E. V. Armbrust, C. Bowler, and B. R. Green. 2007. Chloroplast genomes of the diatoms *Phaeodactylum tricornutum* and *Thalassiosira pseudonana*: Comparison with other plastid genomes of the red lineage. Mol. Genet. Genomics **277**: 427–439. doi:10.1007/s00438-006-0199-4

Padfield, D., G. Yvon-Durocher, A. Buckling, S. Jennings, and G. Yvon-Durocher. 2016. Rapid evolution of metabolic traits explains thermal adaptation in phytoplankton. Ecol. Lett. **19**: 133–142. doi:10.1111/ele.12545

Peñuelas, J., and others. 2013. Human-induced nitrogen-phosphorus imbalances alter natural and managed ecosystems across the globe. Nat. Commun. **4**: 2934. doi:10.1038/ncomms3934

Perelman, A., Z. Dubinsky, and R. Martínez. 2006. Temperature dependence of superoxide dismutase activity in plankton. J. Exp. Mar. Biol. Ecol. **334**: 229–235. doi:10.1016/j.jembe.2006.02.009

Pierrot, D. E., E. Lewis, and D. W. R. Wallace. 2006. MS excel program developed for CO_2 system calculations. Carbon Dioxide Information Analysis Center, Oak Ridge National Laboratory, U.S. Department of Energy.

Prihoda, J., A. Tanaka, W. B. de Paula, J. Allen, L. Tirichine, and C. Bowler. 2012. Chloroplast-mitochondria cross-talk in diatoms. J. Exp. Bot. **63**: 1543–1557. doi:10.1093/jxb/err441

R Core Team. 2022. R: A language and environment for statistical computing. R Foundation for Statistical Computing, https://www.R-project.org/

Rajagopal, S., S. D. S. Murthy, and P. Mohanty. 2000. Effect of ultraviolet-B radiation on intact cells of the cyanobacterium *Spirulina platensis*: Characterization of the alterations in the thylakoid membranes. J. Photochem. Photobiol. B **54**: 61–66. doi:10.1016/s1011-1344(99)00156-6

Ras, M., J. Steyer, and O. Bernard. 2013. Temperature effect on microalgae: A crucial factor for outdoor production. Rev. Environ. Sci. Biotechnol. **12**: 153–164. doi:10.1007/s11157-013-9310-6

Rasdi, N. W., and J. G. Qin. 2014. Effect of N:P ratio on growth and chemical composition of *Nannochloropsis oculata* and *Tisochrysis lutea*. J. Appl. Phycol. **27**: 2221–2230. doi:10.1007/s10811-014-0495-z

Riebesell, U. 2004. Effects of CO_2 enrichment on marine phytoplankton. J. Oceanogr. **60**: 719–729. doi:10.1007/s10872-004-5764-z

Riebesell, U., and others. 2007. Enhanced biological carbon consumption in a high CO_2 ocean. Nature **450**: 545–548. doi:10.1038/nature06267

Rokitta, S. D., and B. Rost. 2012. Effects of CO_2 and their modulation by light in the life-cycle stages of the coccolithophore *Emiliania huxleyi*. Limnol. Oceanogr. **57**: 607–618. doi:10.4319/lo.2012.57.2.0607

Rokitta, S. D., U. John, and B. Rost. 2012. Ocean acidification affects redox-balance and ion-homeostasis in the life-cycle stages of *Emiliania huxleyi*. PloS One **12**: e52212. doi:10.1371/journal.pone.0052212

Rokitta, S. D., S. A. Kranz, and B. Rost. 2022. Inorganic carbon acquisition by aquatic primary producers, p. 81–114. *In* S. C. Maberly and B. Gontero [eds.], Blue planet, red and green photosynthesis. ISTE Ltd. doi:10.1002/9781119986782.ch4

Schoo, K. L., A. M. Malzahn, E. Krause, and M. Boersma. 2013. Increased carbon dioxide availability alters phytoplankton stoichiometry and affects carbon cycling and growth of a marine planktonic herbivore. Mar. Biol. **160**: 2145–2155. doi:10.1007/s00227-012-2121-4

Shi, D., H. Hong, X. Su, L. Liao, S. Chang, and W. Lin. 2019. The physiological response of marine diatoms to ocean acidification: Differential roles of seawater pCO$_2$ and pH. J. Phycol. **55**: 521–533. doi:10.1111/jpy.12855

Siedlewicz, G., A. Żak, L. Sharma, A. Kosakowska, and K. Pazdro. 2020. Effects of oxytetracycline on growth and chlorophyll *a* fluorescence in green algae (*Chlorella vulgaris*), diatom (*Phaeodactylum tricornutum*) and cyanobacteria (*Microcystis aeruginosa* and *Nodularia spumigena*). Oceanologia **62**: 214–225. doi:10.1016/j.oceano.2019.12.002

Stock, W., L. Blommaert, M. De Troch, S. Mangelinckx, A. Willems, W. Vyverman, and K. Sabbe. 2019. Host specificity in diatom-bacteria interactions alleviates antagonistic effects. FEMS Microbiol. Ecol. **95**: fiz171. doi:10.1093/femsec/fiz171

Stoll, M. H. C., K. Bakker, G. H. Nobbe, and R. R. Haese. 2001. Continuous-flow analysis of dissolved inorganic carbon content in seawater. Anal. Chem. **73**: 4111–4116. doi:10.1021/ac010303r

Strickland, J. D. H., and T. R. Parsons. 1972. Practical handbook of seawater analysis. Fisheries Research Board of Canada.

Suzuki, K. 2000. Measurement of Mn-SOD and Cu, Zn-SOD, p. 91–95. *In* N. Taniguchi and J. Gutteridge [eds.], Experimental protocols for reactive oxygen and nitrogen species. Oxford Univ. Press.

Taucher, J., J. Jones, A. James, M. A. Brzezinski, C. A. Carlson, U. Riebesell, and U. Passow. 2015. Combined effects of CO$_2$ and temperature on carbon uptake and partitioning by the marine diatoms *Thalassiosira weissflogii* and *Dactyliosolen fragilissimus*. Limnol. Oceanogr. **60**: 901–919. doi:10.1002/lno.10063

Thangaraj, S., and J. Sun. 2021. Transcriptomic reprogramming of the oceanic diatom *Skeletonema dohrnii* under warming ocean and acidification. Environ. Microbiol. **23**: 980–995. doi:10.1111/1462-2920.15248

Thornton, D. C. O. 2014. Dissolved organic matter (DOM) release by phytoplankton in the contemporary and future ocean. Eur. J. Phycol. **49**: 20–46. doi:10.1080/09670262.2013.875596

Tong, S., D. Xu, Y. Wang, X. Zhang, Y. Li, H. Wu, and N. Ye. 2021. Influence of ocean acidification on thermal reaction norms of carbon metabolism in the marine diatom *Phaeodactylum tricornutum*. Mar. Environ. Res. **164**: 105233. doi:10.1016/j.marenvres.2020.105233

Torstensson, A., M. Hedblom, M. M. Björk, M. Chierici, and A. Wulff. 2015. Long-term acclimation to elevated pCO$_2$ alters carbon metabolism and reduces growth in the Antarctic diatom *Nitzschia lecointei*. Proc. Biol. Sci. **282**: 20151513. doi:10.1098/rspb.2015.1513

Tortell, P. D., C. Payne, C. Gueguen, R. F. Strzepek, P. W. Boyd, and B. Rost. 2008. Inorganic carbon uptake by Southern Ocean phytoplankton. Limnol. Oceanogr. **53**: 1266–1278. doi:10.4319/lo.2008.53.4.1266

Uchiyama, M., and M. Mihara. 1978. Determination of malondialdehyde precursor in tissues by thiobarbituric acid test. Anal. Biochem. **86**: 271–278. doi:10.1016/0003-2697(78)90342-1

Vega-López, A., G. Ayala-López, B. P. Posadas-Espadas, H. F. Olivares-Rubio, and R. Dzul-Caamal. 2013. Relations of oxidative stress in freshwater phytoplankton with heavy metals and polycyclic aromatic hydrocarbons. Comp. Biochem. Physiol. A Mol. Integr. Physiol. **165**: 498–507. doi:10.1016/j.cbpa.2013.01.026

Villanova, V., and others. 2017. Investigating mixotrophic metabolism in the model diatom *Phaeodactylum tricornutum*. Philos. Trans. R. Soc. B **372**: 20160404. doi:10.1098/rstb.2016.0404

Wagner, H., T. Jakob, and C. Wilhelm. 2006. Balancing the energy flow from captured light to biomass under fluctuating light conditions. New Phytol. **169**: 95–108. doi:10.1111/j.1469-8137.2005.01550.x

Wetz, M. S., and P. A. Wheeler. 2007. Release of dissolved organic matter by coastal diatoms. Limnol. Oceanogr. **52**: 798–807. doi:10.4319/lo.2007.52.2.0798

Wiltshire, K. H., M. Boersma, A. Möller, and H. Buhtz. 2000. Extraction of pigments and fatty acids from the green alga *Scenedesmus obliquus* (Chlorophyceae). Aquat. Ecol. **34**: 119–126. doi:10.1023/A:1009911418606

Wolf, K. K. E., E. Romanelli, B. Rost, U. John, S. Collins, H. Weigand, and C. J. M. Hoppe. 2019. Company matters: The presence of other genotypes alters traits and intraspecific selection in an Arctic diatom under climate change. Glob. Change Biol. **25**: 2869–2884. doi:10.1111/gcb.14675

Wu, Y., K. Gao, and U. Riebesell. 2010. CO$_2$-induced seawater acidification affects physiological performance of the marine diatom *Phaeodactylum tricornutum*. Biogeosciences **7**: 2915–2923. doi:10.5194/bg-7-2915-2010

Yakovleva, I. M., A. H. Baird, H. H. Yamamoto, R. Bhagooli, M. Nonaka, and M. Hidaka. 2009. Algal symbionts increase oxidative damage and death in coral larvae at high temperatures. Mar. Ecol. Prog. Ser. **378**: 105–112. doi:10.3354/meps07857

Yoshida, K., I. Terashima, and K. Noguchi. 2007. Up-regulation of mitochondrial alternative oxidase concomitant with

chloroplast over-reduction by excess light. Plant Cell Physiol. **48**: 606–614. doi:10.1093/pcp/pcm033

Young, J. N., S. A. Kranz, J. A. L. Goldman, P. D. Tortell, and F. M. M. Morel. 2015. Antarctic phytoplankton down-regulate their carbon-concentrating mechanisms under high CO_2 with no change in growth rates. Mar. Ecol. Prog. Ser. **532**: 13–28. doi:10.3354/meps11336

Yu, J., X.-X. Tang, P. Zhang, J.-Y. Tian, and H.-J. Cai. 2004. Effects of CO_2 enrichment on photosynthesis, lipid peroxidation and activities of antioxidative enzymes of *Platymonas subcordiformis* subjected to UV-B radiation stress. Acta Botanica Sinica **46**: 682–690.

Zlotnik, I., and Z. Dubinsky. 1989. The effect of light and temperature on DOC excretion by phytoplankton. Limnol. Oceanogr. **34**: 831–839. doi:10.4319/lo.1989.34.5.0831

Conflict of Interest

None declared.